

1                    **HiCAT: A tool for automatic annotation of centromere structure**

2    Shenghan Gao<sup>1,2,#</sup>, Xiaofei Yang<sup>2,3,4,#,\*</sup>, Xixi Zhao<sup>4</sup>, Bo Wang<sup>1,2</sup>, Kai Ye<sup>1,2,4,5,6,\*</sup>

3    <sup>1</sup>School of Automation Science and Engineering, Faculty of Electronic and Information  
4    Engineering, Xi'an Jiaotong University, Xi'an, Shaanxi, China.

5    <sup>2</sup>MOE Key Lab for Intelligent Networks & Networks Security, Faculty of Electronic  
6    and Information Engineering, Xi'an Jiaotong University, Xi'an, Shaanxi, China.

7    <sup>3</sup>School of Computer Science and Technology, Faculty of Electronic and Information  
8    Engineering, Xi'an Jiaotong University, Xi'an, Shaanxi, China.

9    <sup>4</sup>Genome Institute, the First Affiliated Hospital of Xi'an Jiaotong University, Xi'an,  
10    Shaanxi, China.

11    <sup>5</sup>School of Life Science and Technology, Xi'an Jiaotong University, Xi'an, Shaanxi,  
12    China.

13    <sup>6</sup>Faculty of Science, Leiden University, Leiden, The Netherlands.

14    #These authors contributed equally.

15    \*Correspondence: [kaiye@xjtu.edu.cn](mailto:kaiye@xjtu.edu.cn), [xfyang@xjtu.edu.cn](mailto:xfyang@xjtu.edu.cn)

16

## 17 **Abstract**

18 Significant improvements in long-read sequencing technologies have unlocked  
19 complex genomic areas, such as centromeres, in the genome and introduced the  
20 centromere annotation problem. Currently, centromeres are annotated in a semi-manual  
21 way. Here, we propose HiCAT, a generalizable automatic centromere annotation tool,  
22 based on hierarchical tandem repeat mining and maximization of tandem repeat  
23 coverage to facilitate decoding of centromere architecture. We applied HiCAT to human  
24 CHM13-T2T and gapless *Arabidopsis thaliana* genomes. Our results not only were  
25 generally consistent with previous inferences but also greatly improved annotation  
26 continuity and revealed additional fine structures, demonstrating HiCAT's performance  
27 and general applicability.

28 **Keywords:** HiCAT, centromere annotation, long-read sequencing technologies,  
29 gapless genomes

## 30 **Background**

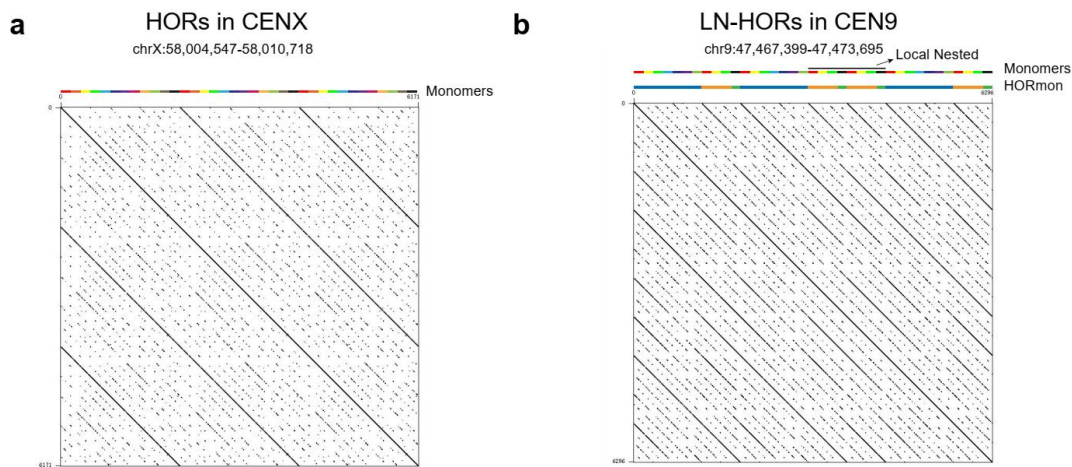
31 Centromeres play an essential role in the transmission of genetic information between  
32 generations. Deep analysis of centromere architecture is critical to understanding  
33 genome stability, cell division and disease development[1]. In most eukaryotes,  
34 centromeres exhibit extra-long tandem repeat (TR) sequences, but the sequence and  
35 length of repeat units, which are referred to as monomers, vary significantly among  
36 species[2]. The canonical order of monomers yields higher order repeats (HORs)[3].  
37 For example, in the active centromere of the human X chromosome (CENX), 12  
38 monomers (the length of one monomer is approximately 171 bp) are consecutively  
39 ordered as HOR units (the length of one HOR unit is approximately  $12 \times 171$  bp) (Fig.  
40 1a)[4]. The sequence identity between monomers within an HOR unit is only 50–90%,  
41 but the pairwise sequence identity between HOR units in a given centromere is as high

42 as 95-100%[5]. The extra-long TRs and high homogeneity make it difficult to achieve  
43 accurate assembly of centromeres, hindering thorough investigations of their sequence  
44 architecture[5]. The rapid development of long read sequencing technologies,  
45 especially PacBio high-fidelity (HiFi) reads, has greatly improved genome assembly  
46 quality[6]. Based on this progress, the Telomere-to-Telomere (T2T) consortium  
47 presented the complete sequence of the human complete hydatidiform mole (CHM) cell  
48 line CHM13 in 2022[7]. In addition, gap-free genome assembly has been achieved in a  
49 few plant genomes, such as those of *Arabidopsis thaliana* and *Oryza sativa*[8, 9].  
50 Significant improvements in genome quality have also contributed to the development  
51 of bioinformatic methods for the study of centromere architecture.

52 Centromere annotation, including monomer inference and HOR detection, is a  
53 prerequisite for studying the structure and evolution of centromeres within and between  
54 species[10]. Previous studies annotated a substantial number of monomers and HORs  
55 in the human genome in a semi-manual manner, facilitating the understanding of  
56 centromere architecture[11-13]. However, this semi-manual method lacks a rigorous  
57 algorithm definition and is time-consuming and laborious, prohibiting its ready  
58 application to new assemblies. To address this question, Dvorkina et al. proposed the  
59 first automatic centromere annotation tool, CentromereArchitect[10], which was based  
60 on StringDecomposer (SD)[4], an algorithm for detecting sequence blocks by taking  
61 monomer templates to decompose centromere DNA sequences. In  
62 CentromereArchitect, monomer inference and HOR detection were considered two  
63 separate problems without interconnections, which often led to biologically inadequate  
64 annotation[14]. The authors next proposed HORmon[14] based on the centromere  
65 evolution postulate (CE postulate, where each monomer appears only once in the HOR

66 unit) to address the lack of interconnection issue in CentromereArchitect. HORmon  
67 first constructs a *de* Bruijn graph based on monomers inferred from  
68 CentromereArchitect and then refines the monomers by considering positional  
69 similarity to amend the graph as a single cycle (referred to as the detected HOR) to  
70 comply with the CE postulate. Finally, HORmon classifies the detected HORs into  
71 canonical and partial HORs. However, the CE postulate has never been strictly proven  
72 and heavily depends on parameters[14], while a single occurrence of each monomer in  
73 a HOR does not always hold. For example, TR expansion does occur within HORs and  
74 forms so-called local nested HORs (LN-HORs) (Fig. 1b). Specifically, human CHM13  
75 CEN9, 13 and 18 have various lengths of HOR units within each chromosome, and  
76 these HORs contain shared monomers (Additional file 1: Fig. S1) due to local nesting,  
77 violating the CE postulate[14]. Thus, a substantial number of partial HORs were  
78 introduced based on the CE postulate, breaking annotation continuity and hindering the  
79 characterization of fine internal architectures in these centromeres (Fig. 1b). To  
80 overcome these problems, we propose a generalizable automatic centromere annotation  
81 tool named HiCAT based on hierarchical tandem repeat mining (HTRM) using a  
82 bottom-up iterative TR compression strategy to detect and represent LN-HORs,  
83 achieving **H**ierarchical **C**entromere structure **A**nno**T**ation. In addition, by maximizing  
84 TR coverage, HiCAT automates parameter selection and optimizes both monomer  
85 inference and HOR detection simultaneously. We applied HiCAT to newly assembled  
86 telomere to telomere (T2T) genomes of human[11] and *Arabidopsis thaliana*[8]. We  
87 compared the results from HiCAT and those from semi-manual and HORmon  
88 approaches. We found that our automated results are generally consistent with those of  
89 previous studies. In addition, HiCAT greatly improved annotation continuity and was

90 able to detect fine structures that were missed by other methods. All the comparison  
91 results demonstrate the superior performance and generalization of HiCAT.



92  
93 **Fig. 1 | Examples of higher-order repeats (HORs).** a. HORs in CHM13 CENX. b.  
94 Local nested HORs (LN-HORs) in CHM13 CEN9. In the monomer tracks, rectangles  
95 in various colours represent different monomers. In the HORmon tracks, differently  
96 coloured rectangles represent different annotations in HORmon. Blue, orange and green  
97 rectangles represent the annotated canonical HORs, partial HORs and monomers not  
98 belonging to any HORs, respectively.

## 99 Results

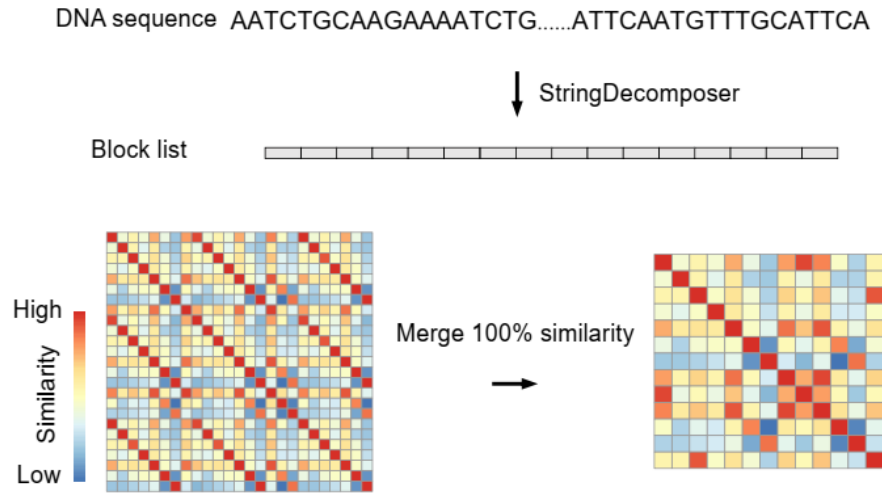
### 100 Overview of HiCAT

101 HiCAT takes a monomer template and a centromere DNA sequence as inputs. There are  
102 two steps in HiCAT: generation of a block list and similarity matrix (Fig. 2a) and mining  
103 of HORs (Fig. 2b). In the first step, HiCAT uses StringDecomposer[4] to transform a  
104 centromere DNA sequence into a block list based on an input monomer template. Each  
105 block is a subsequence of the centromere DNA sequence and exhibits high similarity to  
106 the monomer template. Then, we defined a similarity score based on the block edit  
107 distance to obtain a block similarity matrix (Methods). To improve calculation  
108 efficiency, we pre-processed the block similarity matrix by merging identical blocks. In

109 the second step, to optimize monomer inference and HOR detection at the same time,  
110 we applied a TR coverage maximization strategy to guide parameter selection and  
111 establish feedback between monomer inference and HOR detection. We defined a block  
112 graph whose nodes are blocks and edges are links between any two blocks if their  
113 similarity value is greater than a given similarity threshold. A series of graphs are  
114 created when the similarity threshold iteratively increases from the minimum value (by  
115 default 94%) to nearly 100% with a specific step (by default 0.5%). For each  
116 constructed block graph, we used the Louvain algorithm[15, 16] to detect block  
117 communities, i.e., so-called monomers. We assigned a unique number to each detected  
118 monomer as its ID and transformed the block list into a monomer sequence. To detect  
119 LN-HORs, we proposed the hierarchical tandem repeat mining (HTRM) method  
120 (Methods, Additional file 1: Fig. S2 and Additional file 1: Supplementary method).  
121 HTRM recursively detected and compressed local TRs in the monomer sequence until  
122 no TRs were identified. After HTRM, we merged all TRs with shifted monomer pattern  
123 units, such as 1-2-3-4, 4-1-2-3, 3-4-1-2 and 2-3-4-1, to obtain HORs. We calculated the  
124 associated HOR coverage of each similarity threshold and chose the threshold with the  
125 largest coverage to obtain HiCAT HORs. Finally, we scored HORs based on coverage  
126 and the degree of local nesting to rank all HORs (Methods). Each HOR was named “R  
127 + (rank) + L + (length of HOR unit in the monomer pattern)”. For example, the first  
128 HOR in human CENX with 12 monomers was named R1L12.

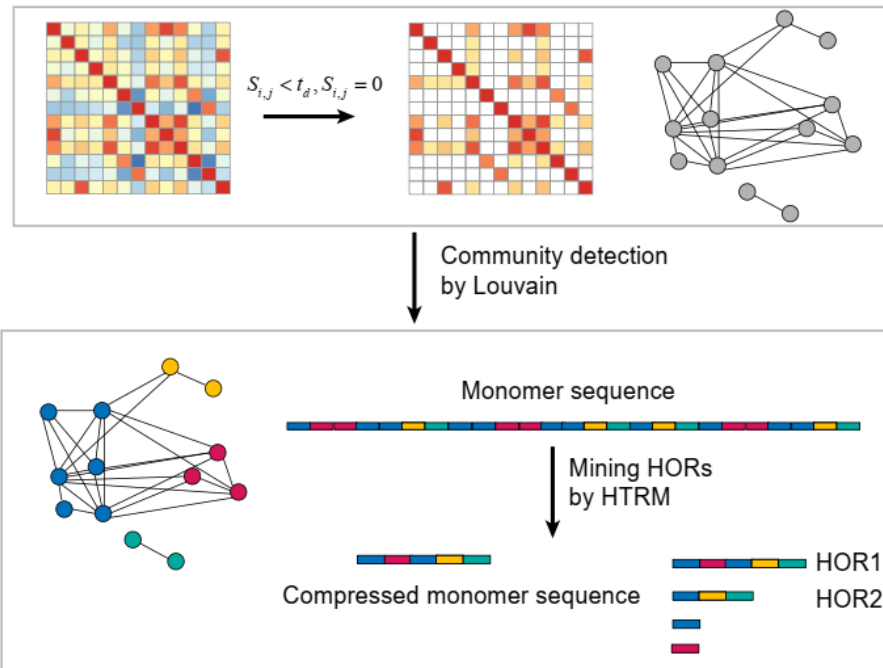
129

**a** Generation of a block list and similarity matrix



**b** Mining higher order repeats

$$t_{d+1} = t_d + step, t_d \in [t_{min}, 100\%)$$



Objective: Maximize tandem repeat coverage

130

131 **Fig. 2 | Overview of HiCAT** **a.** Generation of the block list and similarity matrix. **b.**

132 Mining of higher order repeats (HORs).  $t_d$  represents the similarity threshold in the

133 current iteration.  $t_{d+1}$  represents the similarity threshold in the next iteration.  $t_{min}$  is

134 the minimum similarity threshold. *step* is the threshold increase for each iteration.  
135  $S_{i,j}$  is the similarity between block *i* and block *j*. HTRM: hierarchical tandem  
136 repeat mining. Coloured rectangles in the monomer sequence represent monomers.

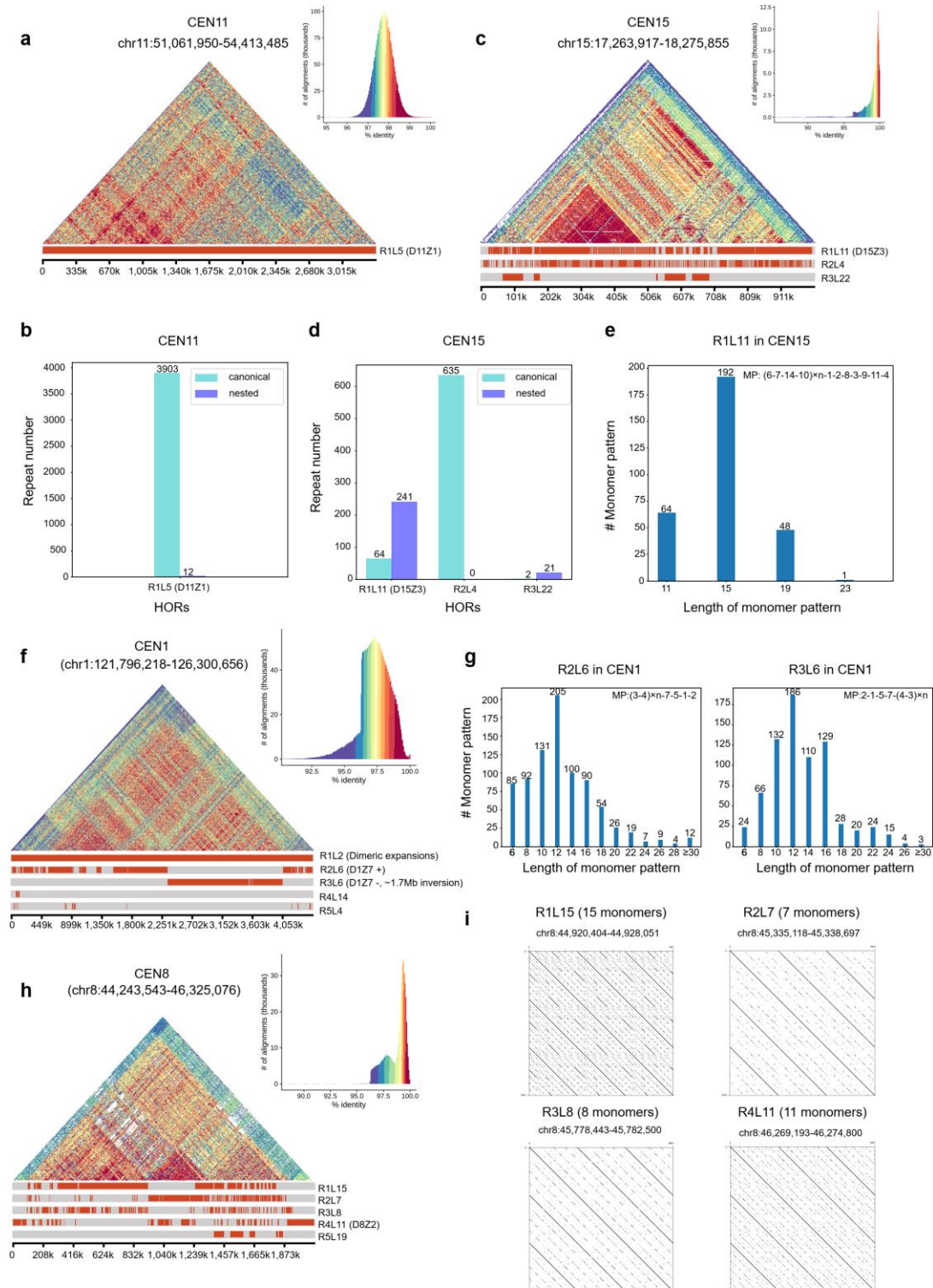
### 137 **Overall performance for human CHM13 centromeres**

138 We first applied HiCAT in an active alpha satellite array for each centromere  
139 (Additional file 2: Table S1) of the human CHM13-T2T genome (v1.0)[11] and  
140 compared the results with published results obtained with semi-manual inference[11,  
141 13]. We found that the HiCAT results were highly consistent with those of previous  
142 studies. The reported HORs in 21 out of 23 centromeres (CEN1, 2, 3, 4, 6, 7, 8, 9, 10,  
143 11, 12, 13, 14, 15, 16, 18, 19, 20, 21, 22 and X) were well detected by HiCAT, while  
144 substantial differences were observed for the remaining two chromosomes, CEN5 and  
145 CEN17 (Additional file 3: Table S2). We first took CEN11 and 15 as examples to further  
146 explore the HiCAT results. There were two types of HOR units, nested (LN-HORs) and  
147 canonical. We found that HORs in CEN11 were rather homogeneous, with as few as 12  
148 nested units in R1L5 (Fig. 3a, b). In CEN15, there were approximately four times as  
149 many nested units in R1L11 as canonical units (Fig. 3c, d). The monomer pattern of the  
150 CEN15 R1L11 unit was (6-7-14-10) $\times$ n-1-2-8-3-9-11-4. Each number represents a  
151 monomer, and “ $\times$ n” represents the number of times that a defined monomer set was  
152 repeated. For example, four consecutive monomers 6-7-14-10 in the R1L11 unit  
153 experienced expansion, and most of them expanded twice, while other numbers of  
154 repeats also existed (Fig. 3e).

155 In CEN1, 8, 9, 10, 13 and 19, previously reported HORs were not ranked first but  
156 among the top five HiCAT results (Additional file 3: Table S2) due to repeat expansion  
157 (Fig. 3 and Additional file 1: Fig. S3). For CEN1, the first HiCAT HOR was R1L2 with



158 two monomers, which was consistent with previously reported dimeric expansions in  
159 D1Z7[13] (the HOR name in previous studies was displayed as “D + chromosome  
160 number + Z + sequential number”[3, 11]). In the CHM13 genome, a 1.7-Mb inversion  
161 in the CEN1 active alpha satellite array[11] split the reported D1Z7 into two HORs,  
162 R2L6 and R3L6 (Fig. 3f), with reversed monomer patterns (3-4-7-5-1-2 and 2-1-5-7-4-  
163 3, respectively) (Fig. 3g). In R2L6 and R3L6, we also detected expansion of two  
164 monomers (3 and 4), and most of them expanded four times (Fig. 3g). The HORs in  
165 CEN8 showed location bias. We detected four frequent HORs, namely, R1L15, R2L7,  
166 R3L8 and R4L11 (Fig. 3h, i), of which R4L11 was consistent with the reported HOR  
167 D8Z2 with 11 monomers[3]. We found that different HORs had different locations in  
168 CEN8. R4L11 was mainly distributed in the marginal area, while R2L7 was enriched  
169 in the centre. R1L15 and R3L8 were distributed between R4L11 and R2L7.



170

171 **Fig. 3| Fine structures in CHM13 CEN11, 15, 1 and 8. a.** Structure and annotation of

172 CEN11. **b.** The numbers of HOR repeats in CEN11. **c.** Structure and annotation of

173 CEN15. **d.** The numbers of HOR repeats in CEN15. **e.** The numbers of monomer

174 patterns in CEN15 R1L11. **f.** Structure and annotation of CEN1. **g.** The number of

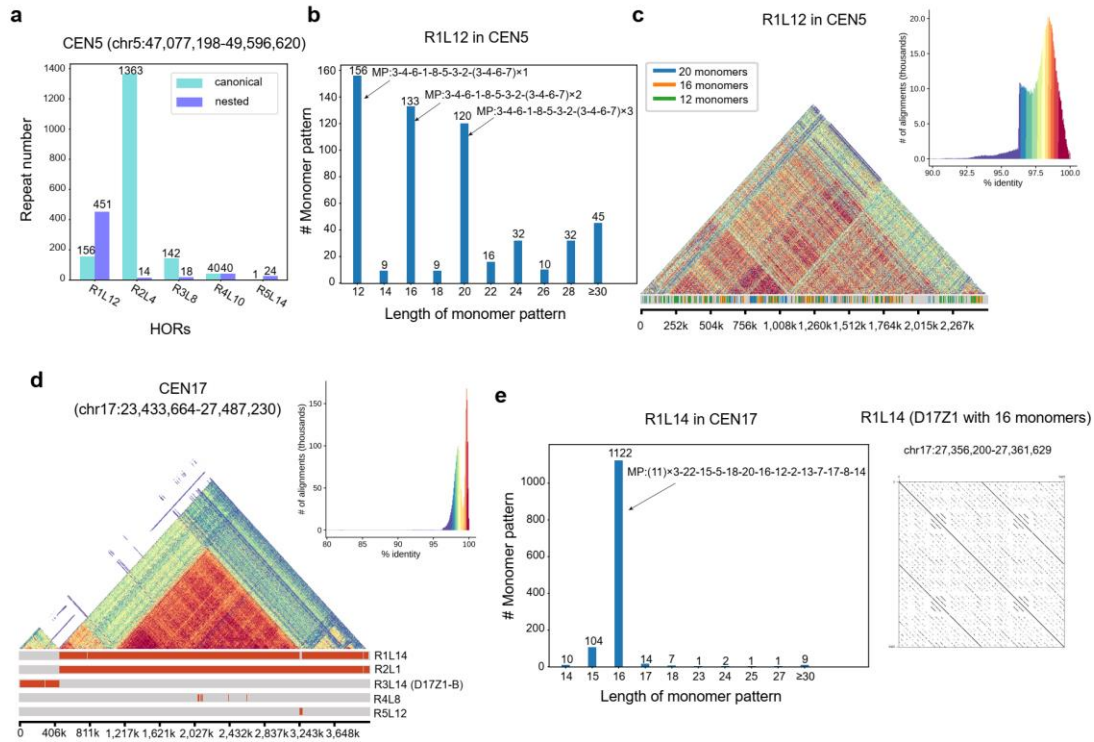
175 monomer patterns in CEN1 R2L6 and R3L6. **h.** Structure and annotation of CEN8. **i.**  
176 Dot plots for different HORs in CEN8. D11Z1, D15Z3, D1Z7 and D8Z2 are previously  
177 reported HORs. MP is the monomer pattern. # means the number of.

### 178 **Substantial differences between HiCAT and semi-manual HOR annotations in** 179 **CEN5 and CEN17**

180 Previous studies have reported that CEN1, 5 and 19 contain shared HORs with six  
181 monomers (D1Z7, D5Z2 and D19Z3) belonging to supra-chromosomal family 1 (SF1)  
182 and are organized as alternating dimers of J1 and J2 monomers[3]. D1Z7 and D19Z3  
183 were detected in CEN1 (R2L6 and R3L6) and CEN19 (R2L6), respectively (Fig. 3f and  
184 Additional file 1: Fig. S3a), while D5Z2 was not detected in the top five HiCAT results  
185 in CEN5 (Additional file 1: Fig. S4a). The top pattern in CEN5 was R1L12, in which  
186 the number of nested units was approximately three times greater than that of canonical  
187 units (Fig. 4a). We found that monomer patterns with lengths of 12, 16 and 20 were the  
188 three most frequent types of patterns, and the specific pattern was 3-4-6-1-8-5-3-2-(3-  
189 4-6-7) $\times$ n with n=1, n=2, and n=3, respectively (Fig. 4b, Additional file 1: Fig. S4b).  
190 Three patterns were distributed in CEN5 without significant location bias (Fig. 4d).

191 Two HORs, D17Z1-B and D17Z1, were reported in CEN17. D17Z1-B with 14  
192 monomers was detected as R3L14 by HiCAT (Fig. 4d), while D17Z1 with 16 monomers  
193 was detected as a special case of R1L14 by HiCAT (Fig. 4e). For R1L14, 1,272 HOR  
194 units were nested with local TRs, while as few as 10 units were canonical (Additional  
195 file 1: Fig. S4c). The monomer pattern was (11) $\times$ n-22-15-5-18-20-16-12-2-13-7-17-8-  
196 14, and most of the units contained 16 monomers with n=3 (Fig. 4e), consistent with  
197 previous reports that D17Z1 belongs to SF3 and experienced triplication of one  
198 monomer, e.g., monomer 11 in R1L14 (Additional file 1: Fig. S4d)[17]. Moreover, we

199 also detected other rarer fine structures of R1L14 with different numbers of monomer  
 200 11 repeats (Additional file 1: Fig. S4e).



201  
 202 **Fig. 4| Resolving centromere structure in CHM13 CEN5 and 17.** a. The HOR repeat  
 203 number in CEN5. b. The number of monomer patterns in CEN5 R1L12. c. Structure  
 204 and annotation of CEN5 for R1L12 with different monomer pattern lengths. d.  
 205 Structure and annotation of CEN17. e. The number of monomer patterns in CEN17  
 206 R1L14 and dot plot for R1L14 (D17Z1) with 16 monomers. D17Z1 and D17Z1-B are  
 207 previously reported HORs in CEN17. MP is the monomer pattern. # means the number  
 208 of.

209 **Comparison with HORmon annotation**

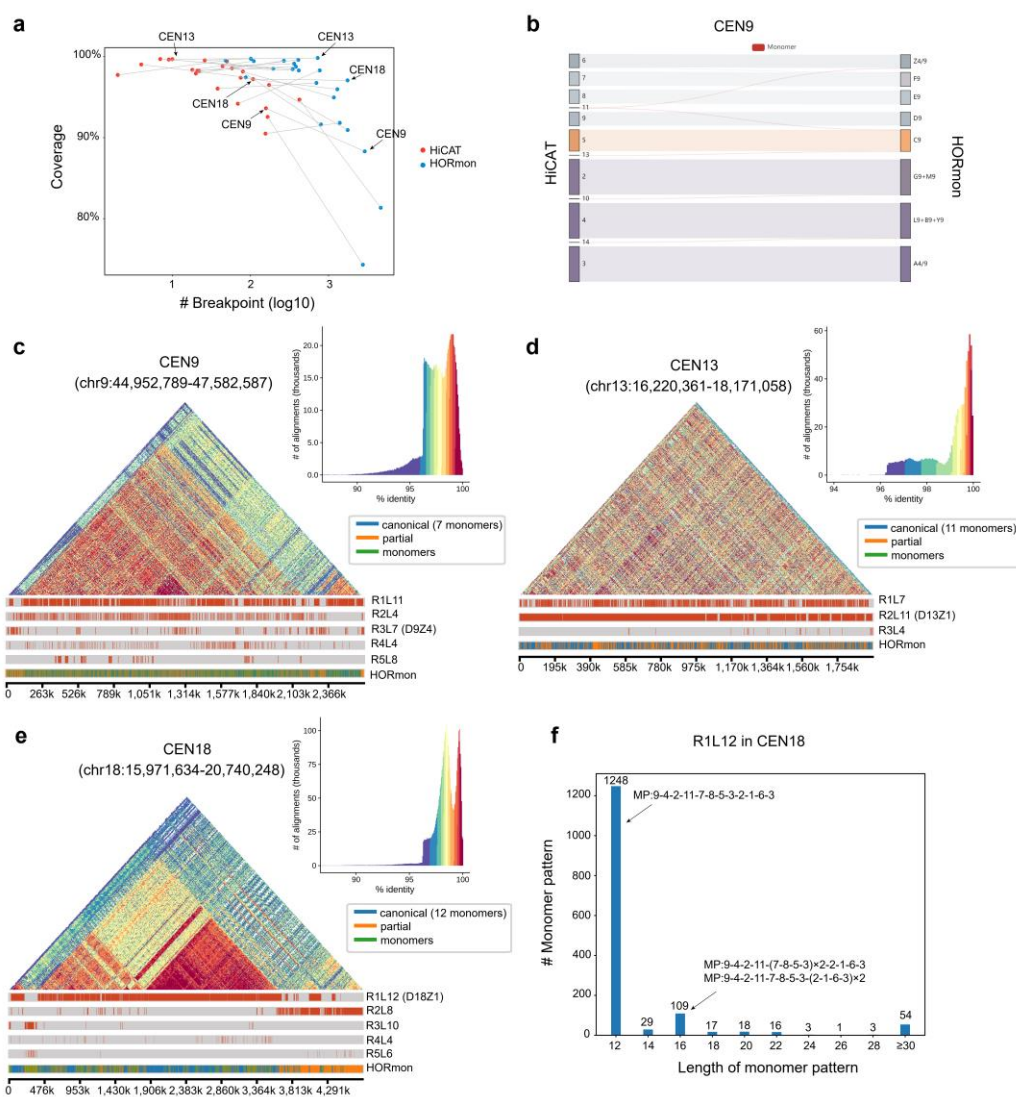
210 We also compared the HORs detected by HiCAT and HORmon[14]. First, we evaluated  
 211 centromere annotation coverage and continuity in all CHM13 centromeres (Additional  
 212 file 4: Table S3) and found that the median coverage of both methods was greater than  
 213 98% (Additional file 1: Fig. S5a). Moreover, we found that HiCAT significantly

214 outperformed HORmon ( $p$ -value =  $4.6e-7$ , Wilcoxon rank sum test) in terms of  
215 continuity, with fewer annotation breakpoints because the LN-HORs were well  
216 captured by HTRM (Fig. 5a and Additional file 1: Fig. S5b).

217 Next, we further compared HiCAT with HORmon in detail by examining CEN9,  
218 13 and 18, which have extensive LN-HORs. Overall, the monomers inferred by the two  
219 methods were largely consistent (Fig. 5b and Additional file 1: Fig. S5c, d). For  
220 example, the frequent monomers inferred by HiCAT and HORmon were consistent in  
221 CEN9 (Fig. 5b) but different in CEN13 monomer 1 and CEN18 monomers 2 and 3 due  
222 to a few-nucleotide difference (Additional file 1: Fig. S5c, d)[14].

223 For HOR detection, HORmon detected canonical HORs with a monomer pattern  
224 as A4/9-(L9+B9+Y9)-C9-D9-E9-Z4/9-(G9+M9) in CEN9[14]. However, monomer F9  
225 with a frequency of 1,193 was annotated as a single monomer in HORmon not  
226 belonging to any HORs, reducing the coverage of HOR annotation. In HiCAT, due to  
227 the HTRM method, monomer 7 (corresponding to monomer F9 in HORmon) was  
228 annotated as a subcomponent of R1L11 with a monomer pattern of (2-3-4-5) $\times$ m-9-8-6-  
229 (2-3-4-7) $\times$ n (Fig. 5c), resulting in an increase in coverage from 88% (in HORmon) to  
230 94% (in HiCAT) (Additional file 1: Fig. S3e). In CEN13 and CEN18, the monomer  
231 patterns of HORs were consistent between HORmon and HiCAT; e.g., D13Z1  
232 (HORmon) equalled R2L11 (HiCAT) in CEN13, and D18Z1 (HORmon) equalled  
233 R1L12 (HiCAT) in CEN18 (Fig. 5d, e). However, nearly half of the regions were  
234 defined as partial HORs or single monomers by HORmon in CEN13 and CEN18  
235 (Additional file 1: Fig. S5e), generating 726 and 1,750 breakpoints, respectively, more  
236 than 10 times the number in HiCAT (Additional file 4: Table S3). We reported more  
237 fine structures of HORs than HORmon. For example, the canonical monomer pattern

238 R1L12 in CEN18 was 9-4-2-11-7-8-5-3-2-1-6-3, and most of the nested units contained  
 239 16 monomers with two expanded parts, 7-8-5-3 or 2-1-6-3 (Fig. 5f, Additional file 1:  
 240 Fig. S5f). Interestingly, we found that the HOR R2L8 in CEN18 with monomer pattern  
 241 9-4-2-11-7-8-5-3 was mainly concentrated on the right end of CEN18, reported as  
 242 partial HORs in the HORmon annotation (Fig. 5e, Additional file 1: Fig. S5g).

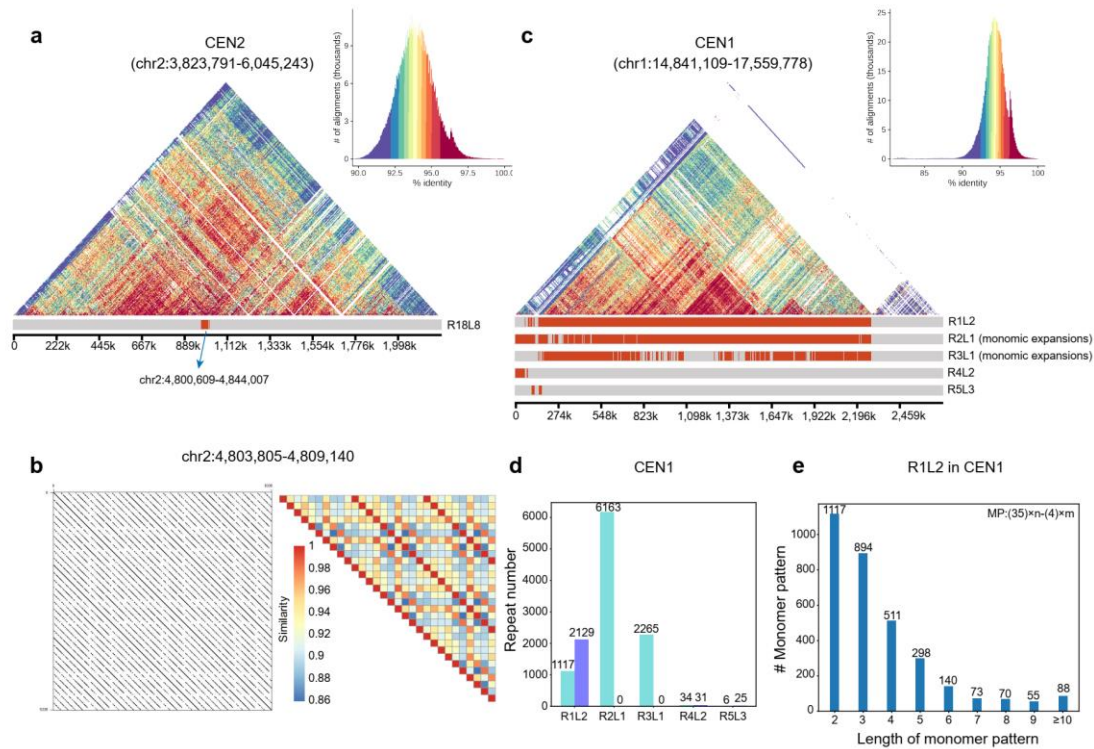


243  
 244 **Fig. 5| Comparison of HOR annotations between HiCAT and HORmon. a.**  
 245 Comparison of the annotation results in terms of coverage and continuity for all CHM13  
 246 centromeres. The line between points links the same centromere annotated by HiCAT  
 247 and HORmon. **b.** Monomer Sankey plot for CEN9 showing the high consistency

248 between the two methods. To display the frequent monomers, we filtered the links with  
249 fewer than 10 matches. The complete Sankey plots are shown in Additional file 1: Fig.  
250 S5h-j. **c-e.** Structure and annotation of CEN9 (c), CEN13 (d), and CEN18 (e) with two  
251 methods. Here, “canonical” represents canonical HORs, “partial” represents partial  
252 HORs, and “monomers” represents monomers that do not belong to any HORs. **f.** The  
253 number of monomer patterns in CEN18 R1L12. D9Z4, D13Z1 and D18Z1 are  
254 previously reported HORs. MP is the monomer pattern. # means the number of.

### 255 **Annotation of centromere structures in the plant genome**

256 To demonstrate generalization of HiCAT, we applied it to *Arabidopsis thaliana* Col-  
257 CEN centromeres assembled by Naish et al.[8]. We first evaluated the accuracy of HOR  
258 annotation by comparing our results with the reported representative HOR region of  
259 chr2:4,808,994-4,826,785[8]. HiCAT detected this HOR as R18L8 (chr2:4,800,609-  
260 4,844,007) with a canonical monomer pattern of 6-4-5-2-6-5-2-4 (Fig. 6a, b, Additional  
261 file 1: Fig. S6, Additional file 5: Table S4). Next, we applied HiCAT to all centromeres  
262 in the Col-CEN assembly (Additional file 2: Table S1, Additional file 4: Table S4). In  
263 contrast to human centromeres, in which most HORs evolved from dimers or  
264 pentamers[17], we found one monomer expansion (monomic expansion) in all  
265 *Arabidopsis thaliana* centromeres (Fig. 6c, Additional file 1: Fig. S7). For example, in  
266 CEN1, the top HOR was R1L2 with canonical pattern 35-4 (Fig. 6c, d), and monomers  
267 35 and 4 experienced a substantial number of expansions (Fig. 6e).



268

269 **Fig. 6| Annotation of centromere structures in *Arabidopsis thaliana* CEN2 and**

270 **CEN1. a.** Structure and annotation of CEN2 R18L8. **b.** Dot plot and similarity heatmap

271 for a part of R18L8. The complete dot plot and similarity heatmap are shown in

272 Additional file 1: Fig. S6. **c.** Structure and annotation of CEN1. **d.** The HOR repeat

273 number in CEN1. **e.** The number of monomer patterns in CEN1 R1L2. MP is a

274 monomer pattern. # means the number of.

## 275 Discussion

276 High-precision and long-read sequencing technologies have revolutionized genome

277 assembly, unlocking complex centromere regions and signalling a new stage in

278 genomics research. The new computing problems introduced by these advances, such

279 as the centromere annotation problem, require novel bioinformatics methods. Here, we

280 propose HiCAT, a generalized computational tool based on the HTRM method and a

281 TR coverage maximization strategy to automatically process centromere annotations.

282 HiCAT is able to correctly annotate HORs and detect fine structures in both human and



283 plant centromeres, especially those with complex LN-HORs. With the emergence of a  
284 large number of high-quality genomes, HiCAT will promote the study of pan-species  
285 centromere diversity and genetic diseases due to defects in centromeres.

286 The efficiency of any computational approach is vital for its success. We ran  
287 HiCAT on a Linux machine with 28 cores (Intel(R) Xeon(R) Gold 6132 CPU @ 2.60  
288 GHz). In all our tests, the maximum runtime was approximately 2 hours for *Arabidopsis*  
289 *thaliana* CEN5, with a length of 2.8 Mb, and the minimum runtime was only 28 seconds  
290 for CHM13 CEN21, with a length of 331 Kb (Additional file 6: Table S5).

291 As promising as HiCAT is, there are still some technical limitations and future  
292 work that we plan to address. The first is the parameter of minimum similarity.  
293 Although we applied a TR coverage maximization strategy to guide selection of the  
294 similarity threshold, some concerns still should be discussed. If the minimum similarity  
295 threshold is set too low, some monomers may be merged, and we may obtain the  
296 ancestral state. If the parameter is set too high, the similarity judgement between blocks  
297 will be too strict, resulting in too many monomers and leading to failure of HOR  
298 detection. In our research, based on a previous study in human centromeres, we set the  
299 minimum similarity threshold as 94% since the similarity between HOR units was  
300 reported to be in the range of 95-100% in humans[5]. For future newly assembled  
301 genomes, this parameter may need to be adjusted to adequately reflect centromere  
302 evolution. Although HOR detection from a fully assembled genome gives us  
303 comprehensive centromere structures, generating a full genome assembly is still a  
304 challenging problem. Annotation of HORs from raw reads is one possible way to obtain  
305 and validate centromere structures, and the method named Alpha-CENTAURI has been  
306 proposed and applied[18, 19]. We will update HiCAT to accept raw reads as input to

307 extend its application scenarios. Finally, hybrid monomers, which are a concatenate of  
308 two or even more monomers, are also important for comprehensively studying  
309 centromere architecture and evolution. Hybrid monomers were hypothesized as the  
310 “birth” of new frequent monomers and were reported in human CEN5 and CEN8[14].  
311 Currently, HiCAT defines monomers based on only the community detection algorithm,  
312 and we will update the monomer inference step to detect hybrid monomers in the future.

### 313 **Conclusions**

314 We have presented a generalized computational tool, HiCAT based on the HTRM  
315 method and a TR coverage maximization strategy to automatically process centromere  
316 annotations. In human and *Arabidopsis thaliana* centromeres, we showed that HiCAT  
317 annotation not only were generally consistent with previous inferences but also greatly  
318 improved annotation continuity and revealed additional fine structures, demonstrating  
319 HiCAT’s performance and general applicability. We believe that with the emergence of  
320 a substantial number of high-quality genomes, HiCAT will promote the study of pan-  
321 species centromere diversity and genetic diseases due to defects in centromeres.

### 322 **Methods**

#### 323 **Datasets in humans and *Arabidopsis thaliana***

324 We obtained active alpha satellite arrays from the complete sequence of the human  
325 CHM13 cell line assembled by the T2T Consortium (version 1.0)[11, 14]. HORmon  
326 annotation of CHM13 centromeres was downloaded from  
327 <https://figshare.com/articles/dataset/HORmon/16755097/2> [14]. We used the Col-CEN  
328 assembly of the *Arabidopsis thaliana* genome and obtained the corresponding  
329 centromere coordinates from Naish et al.[8]. The centromere regions in both CHM13  
330 and Col-CEN are summarized in Additional file 2: Table S1.

### 331 **Generation of the block list and similarity matrix**

332 The first step of HiCAT was to decompose the centromere DNA sequence into the block  
333 list based on the input monomer template by StringDecomposer[4] (Fig. 2a). We  
334 defined the similarity between blocks  $b_1$  and  $b_2$  as:

$$335 \quad 1 - ed(b_1, b_2) / \max(b_1.len, b_2.len) \quad (1)$$

336 where  $ed$  is edit distance between  $b_1$  and  $b_2$ .  $b.len$  is the block length. We  
337 calculated the similarity of each block pair to obtain the similarity matrix. Then, we  
338 merged the identical blocks (similarity = 100%) to obtain the merged similarity matrix  
339 for improving computing efficiency in the HOR mining step.

### 340 **Mining HORs**

341 Based on the merged similarity matrix, we first defined the block graph, whose nodes  
342 are blocks and edges are links between any block pairs if their similarity is greater than  
343 a given similarity threshold. A series of block graphs were constructed based on the  
344 similarity threshold iteratively increasing from the minimum value (by default 94%) to  
345 nearly 100% with a specific step (by default 0.5%). Then, we applied the Louvain  
346 algorithm[15, 16] to detect communities in each graph and considered each detected  
347 community as a monomer. We assigned a unique number to each monomer as its ID.  
348 Next, we transformed the block list into monomer sequences based on block  
349 communities (Fig. 2b). Since local nested TRs hinder the detection of HORs, we  
350 proposed the HTRM method to iteratively detect TRs in monomer sequences. HTRM  
351 includes monomer tandem detection, region checking and sequence updating modules.  
352 The input of HTRM is a monomer sequence with an upper bound for the length of the  
353 TR unit (by default 40 for improving efficiency). We defined a top layer data structure  
354 to record non-overlapping TRs with maximum coverage. First, HTRM applied a

355 monomer TR detection module (Additional file 1: Fig. S2a and Additional file 1:  
356 Supplementary method) to detect new TRs with a given TR unit length. The initial TR  
357 unit length is one. In the second step, we performed region checking (Additional file 1:  
358 Fig. S2b) to check for overlap between newly detected TRs (new TRs) and TRs already  
359 stored in the top layer (old-TRs). The new TRs and old TRs were modified based on  
360 four situations. If there was no overlap between them, the new TRs could be saved in  
361 the top layer directly. If partial overlap was detected between old and new TRs, the  
362 overlapping new-TRs were removed, and the remaining ones were saved in the top  
363 layer. If new TRs covered old TRs, the new TRs replaced old TRs in the top layer.  
364 Finally, if new TRs were covered by old TRs, the new TRs were discarded. In the  
365 sequence updating module, if the top layer was not updated in the region checking step,  
366 the TR unit length for detection was increased by one to redetect TRs. Otherwise, the  
367 monomer sequences of the newly saved TR region were compressed. After compression,  
368 we redetected the TRs by resetting the TR unit length to one. The details and  
369 pseudocode of HTRM are shown in the Additional file 1: Supplementary method. After  
370 HTRM, all detected TRs are reported, and their units are normalized; e.g., units of 4-1-  
371 2-3, 3-4-1-2 and 2-3-4-1 will be normalized as 1-2-3-4. Then, we merged TRs with the  
372 same ordered set of normalized units as a HOR. We calculated the associated HOR  
373 coverage of each similarity threshold and chose the threshold with the largest coverage  
374 for defining HiCAT HORs. Finally, we ranked HiCAT HORs by HOR score combining  
375 the coverage and the degree of local nesting. The HOR score is defined as:

$$376 \quad \text{HORscore} = cr * pr \quad (2)$$

$$377 \quad cr = \text{HOR.len} / m.\text{len} \quad (3)$$

$$378 \quad pr = \text{HOR.rn} / (\text{HOR.len} / \text{HORunit.len}) \quad (4)$$

379 where  $cr$  is the coverage for the HOR in the input monomer sequence.  $pr$   
380 represents the degree of local nesting.  $HOR.len$  is the length of the HOR region in the  
381 monomer pattern, and  $m.len$  is the length of the monomer sequence.  $HOR.rn$  is the  
382 repeat number for the HOR, and  $HORunit.len$  is the length of the HOR unit in the  
383 monomer pattern. If the HOR is over-compressed, which means that it contains only a  
384 small number of repeats but with high coverage,  $HOR.rn$  will be significantly smaller  
385 than  $HOR.len / HORunit.len$ , and  $pr$  will balance the coverage and nested degree of  
386 the HOR. We named each HOR in each chromosome as “R + (ranking) + L +  
387 ( $HORunit.len$ )”. For example, in human CEN11, the first HOR is R1L5.

### 388 **Annotation visualization**

389 StainedGlass[20] was used to visualize the TR structures with identity heatmaps, and  
390 the window size was set to 2000. We used Gepard[21] to create dot plots. For HiCAT  
391 results, within each centromere, we visualized the top five HORs with repeat numbers  
392 greater than 10 and reported all detected HORs in the output files.

### 393 **Abbreviations**

394 HiCAT: hierarchical centromere annotation tool

395 CHM: complete hydatidiform mole

396 T2T: Telomere-to-Telomere

397 TR: tandem repeat

398 HOR: higher order repeat

399 CEN: centromere

400 HiFi: high-fidelity

401 SD: StringDecomposer

402 CE postulate: centromere evolution postulate

403 LN-HOR: local nested higher order repeat

404 HTRM: hierarchical tandem repeat mining

405 **Ethics approval and consent to participate**

406 Not applicable.

407 **Consent for publication**

408 Not applicable.

409 **Availability of data and materials**

410 Datasets used for the analyses in this study are summarized in Additional file 3: Table

411 S2. The source code of HiCAT and all annotation results are publicly available at

412 <https://github.com/xjtu-omics/HiCAT>.

413 **Competing interests**

414 The authors declare that they have no competing interests.

415 **Funding**

416 This work is supported by National Science Foundation of China (32125009, 62172325,

417 32070663), by the Fundamental Research Funds for the Central Universities, by the

418 Natural Science Basic Research Program of Shaanxi (2021GXLH-Z-098), the Science

419 and Technology Project of Xi'an (No. 21RGSF0013), by Key Construction Program

420 of the National “985” Project.

421 **Authors' contributions**

422 KY and XY conceived the study. SG, BW and XZ analysed the data. SG and XY

423 developed the program. SG and XY wrote the manuscript. SG completed figures of

424 manuscript. All authors read and approved the final manuscript.

425 **Acknowledgements**

426 The authors thank Yujing Liu and Peng Jia for their important suggestions and feedback.

## 427 **References**

- 428 1. McKinley KL, Cheeseman IM: **The molecular basis for centromere identity**  
429 **and function.** *Nat Rev Mol Cell Biol* 2016, **17**:16-29.
- 430 2. Henikoff S, Ahmad K, Malik HS: **The centromere paradox: stable**  
431 **inheritance with rapidly evolving DNA.** *Science* 2001, **293**:1098-1102.
- 432 3. McNulty SM, Sullivan BA: **Alpha satellite DNA biology: finding function**  
433 **in the recesses of the genome.** *Chromosome Res* 2018, **26**:115-138.
- 434 4. Dvorkina T, Bzikadze AV, Pevzner PA: **The string decomposition problem**  
435 **and its applications to centromere analysis and assembly.** *Bioinformatics*  
436 2020, **36**:i93-i101.
- 437 5. Bzikadze AV, Pevzner PA: **Automated assembly of centromeres from ultra-**  
438 **long error-prone reads.** *Nat Biotechnol* 2020, **38**:1309-1316.
- 439 6. Wenger AM, Peluso P, Rowell WJ, Chang PC, Hall RJ, Concepcion GT, Ebler  
440 J, Functammasan A, Kolesnikov A, Olson ND, et al: **Accurate circular**  
441 **consensus long-read sequencing improves variant detection and assembly**  
442 **of a human genome.** *Nat Biotechnol* 2019, **37**:1155-1162.
- 443 7. Nurk S, Koren S, Rhie A, Rautiainen M, Bzikadze AV, Mikheenko A, Vollger  
444 MR, Altemose N, Uralsky L, Gershman A, et al: **The complete sequence of a**  
445 **human genome.** *Science* 2022, **376**:44-53.
- 446 8. Naish M, Alonge M, Wlodzimierz P, Tock AJ, Abramson BW, Schmucker A,  
447 Mandakova T, Jamge B, Lambing C, Kuo P, et al: **The genetic and epigenetic**  
448 **landscape of the Arabidopsis centromeres.** *Science* 2021, **374**:eabi7489.
- 449 9. Song JM, Xie WZ, Wang S, Guo YX, Koo DH, Kudrna D, Gong C, Huang Y,  
450 Feng JW, Zhang W, et al: **Two gap-free reference genomes and a global**  
451 **view of the centromere architecture in rice.** *Mol Plant* 2021, **14**:1757-1767.
- 452 10. Dvorkina T, Kunyavskaya O, Bzikadze AV, Alexandrov I, Pevzner PA:  
453 **CentromereArchitect: inference and analysis of the architecture of**  
454 **centromeres.** *Bioinformatics* 2021, **37**:i196-i204.
- 455 11. Altemose N, Logsdon GA, Bzikadze AV, Sidhwani P, Langley SA, Caldas GV,  
456 Hoyt SJ, Uralsky L, Ryabov FD, Shew CJ, et al: **Complete genomic and**  
457 **epigenetic maps of human centromeres.** *Science* 2022, **376**:eabl4178.
- 458 12. Shepelev VA, Uralsky LI, Alexandrov AA, Yurov YB, Rogaev EI, Alexandrov  
459 IA: **Annotation of suprachromosomal families reveals uncommon types of**  
460 **alpha satellite organization in pericentromeric regions of hg38 human**  
461 **genome assembly.** *Genom Data* 2015, **5**:139-146.
- 462 13. Uralsky LI, Shepelev VA, Alexandrov AA, Yurov YB, Rogaev EI, Alexandrov

- 463            **IA: Classification and monomer-by-monomer annotation dataset of**  
464            **suprachromosomal family 1 alpha satellite higher-order repeats in hg38**  
465            **human genome assembly.** *Data Brief* 2019, **24**:103708.
- 466    14.    Kunyavskaya O, Dvorkina T, Bzikadze AV, Alexandrov IA, Pevzner PA:  
467            **Automated annotation of human centromeres with HORmon.** *Genome Res*  
468            2022, **32**:1137-1151.
- 469    15.    Blondel VD, Guillaume J-L, Lambiotte R, Lefebvre E: **Fast unfolding of**  
470            **communities in large networks.** *Journal of Statistical Mechanics: Theory*  
471            *and Experiment* 2008, **2008**.
- 472    16.    Traag VA, Waltman L, van Eck NJ: **From Louvain to Leiden: guaranteeing**  
473            **well-connected communities.** *Sci Rep* 2019, **9**:5233.
- 474    17.    Alexandrov I, Kazakov A, Tumeneva I, Shepelev V, Yurov Y: **Alpha-satellite**  
475            **DNA of primates: old and new families.** *Chromosoma* 2001, **110**:253-266.
- 476    18.    Sevim V, Bashir A, Chin CS, Miga KH: **Alpha-CENTAURI: assessing novel**  
477            **centromeric repeat sequence variation with long read sequencing.**  
478            *Bioinformatics* 2016, **32**:1921-1924.
- 479    19.    Suzuki Y, Myers EW, Morishita S: **Rapid and ongoing evolution of**  
480            **repetitive sequence structures in human centromeres.** *Sci Adv* 2020, **6**.
- 481    20.    Vollger MR, Kerpedjiev P, Phillippy AM, Eichler EE: **StainedGlass:**  
482            **Interactive visualization of massive tandem repeat structures with**  
483            **identity heatmaps.** *Bioinformatics* 2022.
- 484    21.    Krumsiek J, Arnold R, Rattei T: **Gepard: a rapid and sensitive tool for**  
485            **creating dotplots on genome scale.** *Bioinformatics* 2007, **23**:1026-1028.
- 486